JOURNAL OF OPTOELECTRONICS AND ADVANCED MATERIALS Vol. 12, No. 1, January 2010, p. 146 - 151

Interferometric patterning of the azo-polymers surface

V. DAMIAN*, I. APOSTOL, N. HURDUC[a]
National Institute for Lasers Plasma and Radiation Physics, Atomistilor 409, PO Box MG-36, Măgurele 077125, Ilfov, România
[a]*Technical University of Iasi, Department of Natural and Synthetic Polymers, Bd.Mangeron 71, 700050-Iasi, Romania*

Direct patterning of the polymeric surface, using a Talbot interferometer, was the solution for nanostructuring the polymers using UV short coherence laser radiation. Using the 355 nm radiation from a Nd:YAG laser, as a light source, a more flexible and controllable setup, was developed for direct patterning of azopolymer films by interference. With a grating like beam splitter we used the interference of (0, +1) or (+1,-1) diffraction orders to obtain an interference pattern. The two beams are superimposed using two parallel mirrors. In this way, controllable patterns having variable grating pitch can be obtained. The article describes the setup and some surface patterning results obtained on an azo-polymer (polysiloxane modified with azobenzene and naphthalene).

(Received December 15, 2009; accepted January 20, 2010)

*Keywords: I*nterferometric patterning, Nanostructures, UV wavelength, Gratings, Azo-polymers

1. Introduction

Three-dimensional surface structuration under the action of UV laser radiation is an important step in the azo-polymer application in MEMS, bio and chemical sensors. The process is based on the photochromic properties of some azo-polymers [1, 10]. One way to pattern, the polymer surface is to expose it at a light field created by a Talbot interferometer, at fluences smaller than the ablation threshold. Under ablation threshold processing assure the preservation of polymer properties. The advantage is that this kind of interferometer overcomes the coherence problems, important especially for deep UV. Unfortunately that type of interferometer introduces some other inconvenient: difficulties to manipulation, necessity of a protection of the grating with a fused silica sheet, not a direct control of the interfering beams, and secondary multiple beams. Those problems are overcome with a more flexible new interferometric setup, a two beams interferometer [2, 3] using as a beam splitter a diffraction grating.

2. Experimental set-up

To obtain an interference field with a selective and controlled interfrange we use the set-up scheme from (fig.1). The laser beam is incident on a grating and is diffracted. To obtain the interference pattern we use only the ±1 and 0 diffraction orders that are superposed. The beams are used in pair (+1, 0) or (-1, +1), that can be selected with a beam selector (S).

The diffracted beams are separated by an angle θ_k according with[3]:

$$\sin \theta_k = k \cdot \lambda / g;$$

where: k – diffraction order, g- the grating pitch, λ – wavelength.

The pitch, of the induced surface structure, is correlated with the interference light field which is incident on azopolymeric film surface and is equal with:

$$i = \lambda/(2 \cdot n \cdot \sin(\alpha/2));$$

where: i – the interfrange, n – refraction index of the medium, and α - the angle between the interfering beams ($\alpha = \theta$ or 2θ). In the case of two beams at θ angle, an interferometric image with the pitch equal with the pitch of the diffraction grating is obtained and in case of two beams separated by 2θ angle, the pitch is half the diffraction grating pitch.

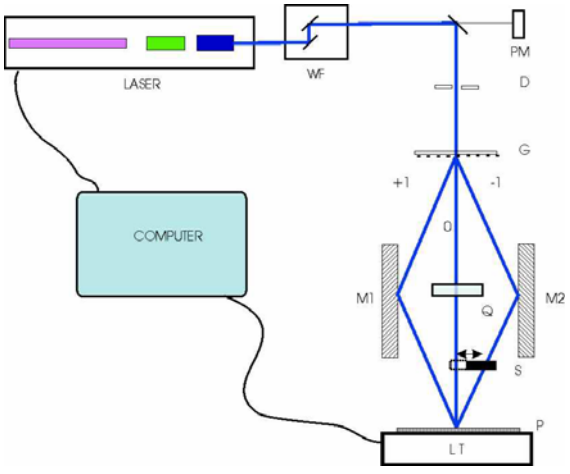

Fig. 1. Interferometric set-up scheme: Nd:YAG laser, WF- wavelength filter, PM - energymeter, D – aperture, G - diffraction grating, M1,2 - kinematics mirrors, Q – fused silica phase compensator, S – beam selector, P – sample, LT – translation stage.

To superpose the diffracted beams, we use a pair of kinematic mirrors (M1, M2) that can be tuned according with the desired interference pitch grating and miss-alignments compensation. To compensate the phase difference between the beams, in case of (+1, 0) diffraction orders interference, we have used a fused silica plate (Q) introduced in the zero order beam pathway.

The light field in the interference zone, of the two beams, will be a sinusoidal type and can be described by:

$$I(\mathrm{P}) = I_1 + I_2 + 2\left(I_1 I_2\right)^{1/2} |\gamma| \cos(\Delta\phi)$$

where: $\Delta\phi$ - the phase difference between the interfering fields, γ – the coherence factor, and $I_{1,2}$ - represents the intensity of the two interfering beams.

The main advantage of this set-up is the possibility to know and to control the energy of the interfering beams and consequently the fluence of the laser field incident on the sample. For this, the laser energy was permanently monitored by an energy meter (PM).

The factor that will characterize the shape of the patterned grating (beside the polymers response) will be the fringes visibility. The fringe visibility is defined by:

$$V = \frac{2\rho}{1+\rho^2}$$

where: $\rho = I_1/I_2$, $I_{1,2}$ - represents the intensity of the two interfering beams.

The irradiated sample is an azo-polymer film (P) which can be moved with a linear translation stage (LT) (Thorlabs-150 mm travel, motorized linear stage with a precision of 5 μm at a resolution of 0.1 μm) in front of the interference field. Specialized program assures computer control of the linear translation stage and the irradiations parameters (energy and number of pulses).

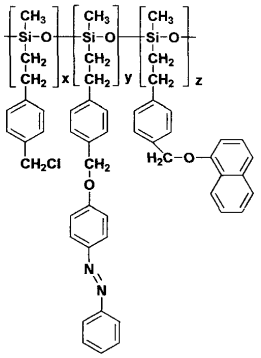

Fig. 2. The chemical probe structure: polysiloxan modified with 68% azobenzen and 14% naphthalene.

The azo-polymeric materials are based on polysiloxanic chains, modified with azobenzenic groups [3]. Two types of applications are possible: immobilization and laser nano-manipulation of biomolecules on the film surfaces and directional cells growth on the nanostructured surfaces. The azo-polymer (Fig. 2), used in our experiment, was a polysiloxane modified with 68% azobenzen and 14% naphthalene. The naphtalene has no direct role in the photoisomerization process, but it can interact with the azobenzene group, and influence the nanostructuring.

The absorption spectrum for a great number of azopolysiloxanes evidenced a maximum for the absorption spectrum in a region around of a wavelength of 350 nm, but also a tendency for higher absorption maxima at wavelengths lower than 200 nm.

It is possible that a mechanism based on conformational instability state, generate a fluid phase during UV/VIS irradiation. [1, 4, 10] This special state is a consequence of the continuous azobenzene groups *trans-cis-trans* photo-isomerization processes, which may be accompanied, as a function of chemical structure, by strong dipole-moment fluctuations along the chain [4]. If the azobenzene group is connected in the polymeric main- or side-chain, these modifications will impose conformational changes on the entire polymeric chain level, accompanied by strong dipole-moment fluctuations along the chain. This continuous photo-isomerization motion of the azo-groups induces a conformational instability on the entire polymeric chain that hinders the phase stabilization in a solid state.

The high response speed of the azobenzenic groups at UV irradiation in the solid state comparing with the solution may be explained by the flexibility of the main chain with a polysiloxanic structure and by the amorphous film structure that assures a high free volume [1, 5, 6]. The cis–trans azobenzenic groups relaxation phenomena can take place thermal-activated only (in dark) but in this case the processes are much slower (in a time scale of days). Therefore, a big difference in the film surface response can be expected if the operational conditions are modifie d (presence or absence of visible light during UV irradiation).

2. Experimental results

The light source, of our set-up, was a Nd:YAG laser working on his third harmonic at 355 nm (Continuum – Surelite II). The laser has a pulse length at FWHM of 5ns, with a repetition frequency of 10 Hz and a beam divergence of 0.6 mrad. Using the possibility to select the energy of the output beam, by changing the Q-switch delay settings of the Pokels cell in the domain (0.9 ÷ 1.8) μs, we have obtained a domain of (3 ÷ 140) mJ for a constant value of the tension of the flash lamp (1.36kV) at optimum for maximum energy.

The beam divider, that we have used, was a 1μm diffraction grating (phase mask) from UV grade fused silica (Ibsen Photonics) that give us a diffraction angle of $\theta_k \sim 0.363$ rad at 355nm.

As we have shown, the shape of the induced patterns will be defined by the fringe visibility. To evaluate this, we have analyzed (Table 1) the rate between the energy in diffracted beams after the diffraction grating, and after the

pass from optical elements and the incident energy on the diffraction grating.

Table 1. Interfering beams characteristics rated with the incident beam.

Diffraction orders	±1	0
Grating efficiency	28%	22%
Incident energy rate after:	Reflection 26.9%	Transmission 20%

According with our intensity rate figures and interference scheme, the visibility of the obtained franges will be $V \sim (1$ or $0.96)$, that means good sinusoidal fringes with only a small "offset" of 4% in the case of (+1, 0) interference.

The azopolymer modified with naphtalene used in experiments present a strong absorption spectrum at the working wavelength (vertical line 355 nm) (Fig.3). Transmission has been measured with a Perkin Elmer UV/VIS spectrometer.

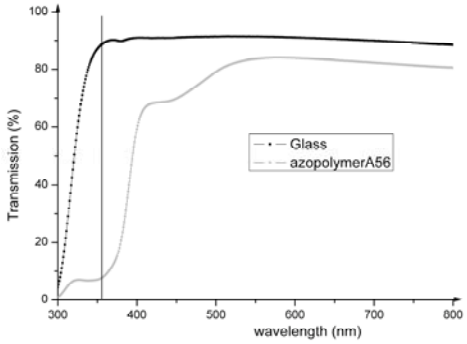

Fig. 3. Transmission spectrum of the azopolymer with naphtalene (named A56) and the glass support spectrum (relative to air).

The relief modulated surface obtained on different irradiation condition were analised and measured with: a Zeiss Optical Microscope (Imager. Z1m), with an AFM (Park System XE - 100), and with a white light interferometer (WLI) microscope (Ambios Xi - 100).

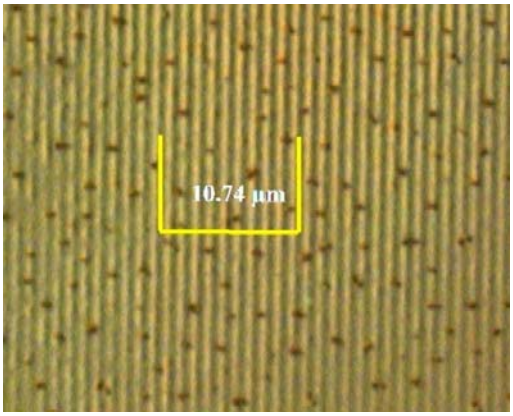

Fig. 4. A 1µm pitch grating; irradiation conditions: incident fluence: 0.016 J/cm^2 and 400 pulses.

The experimental setup was utilized in a relatively symmetrical alignment that allow us to obtain a pitch of (1.06 ± 0.05) µm (Fig. 4) for the (+1, 0) diffraction orders interference, and a pitch of (0.49±0.05) µm (Fig. 5) for the (+1, -1) diffraction orders interference, from the 1µm diffraction grating, used like the beam divider.

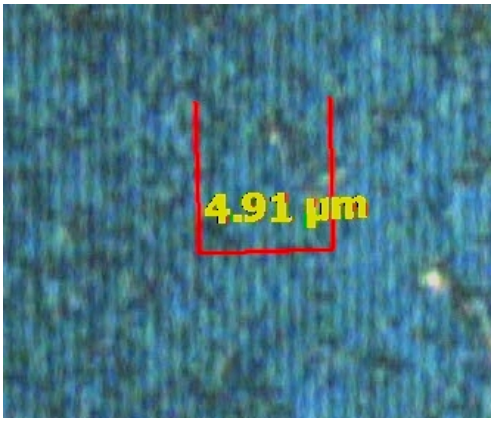

Fig. 5. A 0.5µm pitch grating obtained at a incident fluence, of 0.011 J/cm^2) and 400 pulses.

The microscope analyses of the induced structure (Fig. 4) were completed with the AFM investigation (Fig. 6) and the WLI investigation (Fig. 7). This procedure put in evidence the thick irregularities of the obtained gratings, due to non-uniformity of the polymer film but also the depth of the surface relief gratings.

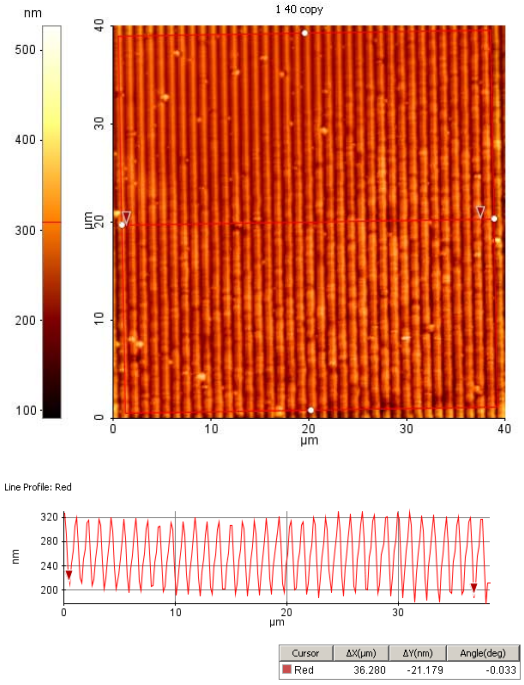

Fig. 6. Atomic Force image and profile of a 1µm grating induced pattern; irradiation conditions: 0.016 J/cm^2 and 400 pulses.

The modulation depth vary in the domain of (10 ÷ 200) nm, according to the number of pulses and fluence. The surface relief gratings obtained profiles are nearly sinusoidal.

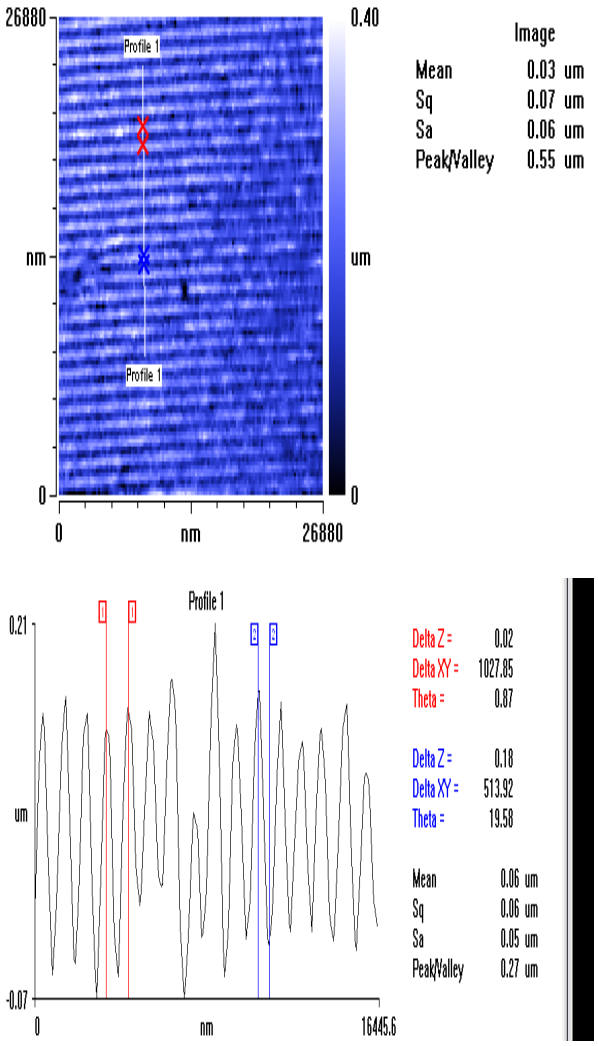

Fig. 7. WLI image and profile of the 1µm induced grating; iradiation conditions: 0.016 J/cm^2 and 400 pulses.

The results obtained for surface modulation under the action of laser radiation in this case are commented in (Table 2). They look similar with the results obtained in case of other azopolymeric films [9].

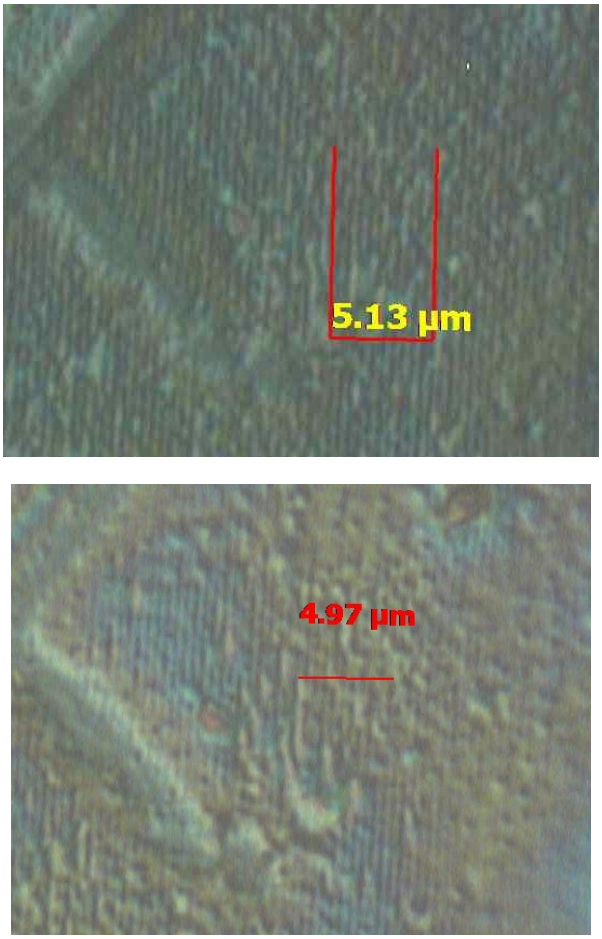

Fig. 8. Time evolution of a 500 nm pitch grating (irradiation conditions: 30 pulses @ 0,08 J/cm^2 fluence) immediately after the patterning and after 3 month. The probe was kept at room temperature (21-30)^0 C.

Even the naphthalene has no role in photoizomerization trans-cis process it may influence it from the point of view of time stability. This can be demonstrated by the good initial structures obtained and relatively slow evanescence of them, according with the initial laser beam fluence. The time stability of the induced structure is about 120 hours for the irradiation conditions with incident fluence of 0.016 J/cm^2 and 400 pulses (Fig. 8).

All experiences realized on the azopolimer with naphtalene where summarized in Table 2, from the point of view of: fluence, number of pulses, obtained structures and time evolution after the irradiations.

Table 2. Characterization of obtained structures as a function of incident fluence and pulse number.

Interference between (±1) diffraction orders Expected pitch: 0.5 μm; obtained pitch: 0,49±0.05 μm							
Fluence (J/cm^2)	0.01614	0.03228	0.04842	0.0807	0.1076	0.1345	0.15064
No. of pulses	400	150 - 500	30 - 300	6 - 100	10 - 500	1 - 50	1 - 30
Irradiation effects.	Appears the surface modulation as surface relief grating	Good surface relief grating	Good surface relief grating	Good surface relief grating	Good surface relief grating. For more 150 appear "burned" zones	Over exposing, with zones without grating.	Burned zones with small zones with gratings.
Time evolution	After 20 days the surface patterning dissapears	After 3 month slightly visible gratings	After 3month only low contrast SRG are visible	See Fig. 8 After 3month it can be seen still the good contrast gratings .	Up to 100 the grating pattern is stable. Over 150 it appeared an over "exposed", white zone, and even not an image at 500.	Over exposing and slightly visible gratings for small no. of pulses.	Over exposing with slightly visible grating.
Interference between 1 and 0 diffraction orders Expected pitch: 1 μm; obtained pitch: 1.08±0.05 μm							
Fluence (J/cm^2)	0.0141	0.0282	0.0423	0.0705	0.094	0.1175	0.1316
No. of pulses	250 - 400	150 - 400	200 - 300	50 - 200	25 - 100	5 - 50	5 - 50
Irradiation effects.	100 pulses is a threshold value. For higher number of incident pulses low contrast gratings appear.	Over 200 incident pulses, good contrast gratings are obtained.	Good patterns but for bigger no. of pulses, some overheated regions are present.	Over heating zone but some good patterns.	Overheating, only some zone modulated.	Good gratings. It seems they were obtained by ablation.	It seems it was obtained an ablated grating.
Time evolution	Over the threshold seems to be some changes.	Resistant in time gratings	Resistant in time gratings	Resistant in time gratings No change in aspect.	Resistant in time gratings No change in aspect	Resistant in time. No modification.	Resistant in time. No modification.

Looking in the Table 2 we can conclude that the 500 nm grating can be obtained for a domain from 0.08 J/cm^2 and (50-150) pulses to 0.11 J/cm^2 and (10 - 100) pulses. Outside this domain we have not enough energy or too much energy. Comparing with the necessary energy for 1000 nm pitch grating (0.033 J/cm^2 and (200 -500) pulses – 0.0705 J/cm^2 (up to 200 pulses)) J/cm^2 , we can see we

need less energy for writing a 1 μm grating and those are more stable in time.

The low fluence, for which the structuration was observed, evidences that the mechanism responsible for the surface relief gratings formation is an inner material reorganization and not the material ablation. [7, 9, 10]

We have evaluated the obtained gratings even from the point of view of the grating efficency. Table 3 presents the medium efficiency of diffraction orders, for 325 nm at 11 mW of a CW HeCd laser (Kimmon Electric). The efficency was calculated as the ratio between the diffracted beam (I_k) and the incident one (I).

Table 3. The medium efficency of obtained gratings.

Grating pitch	Difraction efficiency (I_k /I)		
	0	1	2
1000nm	0.092801	0.012462	0.003215
500nm	0.253732	0.004862	*it could not be measured, the diffraction angle is too big.

It can be seen the resulting gratings have different efficencies from the original, that are presented in table 1. While the 1 μm patterned grating has an equilibrated output of 0, ±1 orders, the 0.5 μm gratings has only a small output in ±1 orders. Both of the induced patterns are less efficient than the master that can be explained by the fact that the master is a phase mask, while the induced ones are amplitude gratings. The diffraction efficiencies of the various orders diffracted by the grating were fitted to theoretical predictions corresponding to various structure models of the gratings. The fitting procedure was used to provide the parameters of the gratings, such as the width, the grating height, the pitch or shape factors [8].

3. Conclusions

We have developed a versatile tool for surface patterning different kind of materials. In the same time, the experimental set-up, gives us the possibility to control all the interesting experimental parameters: fluence of the interfering beams, number of pulses and angle between the interfering beams and consequently the patterned grating pitch.

The surface structuration evolution of azopolimer naphtalene modified is similar with other azopolymer films that we have studied. The structuration time depends on the incident laser fluence and of pulses number: from 1 pulse up to 500 pulses (of 5 ns each).

Taking into account the fast response of the material at the UV irradiation it can be considered that the surface relief formation is due to a spontaneous reorientation of the molecules due to the conformational changes as a result of the isomerisation process.

In the same time we have observed that we have a small fluence domain to obtain good relief but but different for structuring for the two realized gratings pitch.

The naphthalene influenced the stability of the obtained structures, in the way that only some of the 500 nm gratings where reversible in time.

References

[1] P. Karageorgiev, D. Neher, B. Schulz, B. Stiller, U. Pietsch, M. Giersig, L. Brehmer, Nature Materials **4** , 699 (2005).
[2] P. Rochon, E. Batalla, A. Natansohn, Appl. Phys. Let. **66**(2) (1995).
[3] A. Kassu, J.-M. Taguenang, A. Sharma, Applied Optics **46**(4), 489 (2007).
[4] N. Hurduc, R. Enea, D. Scutaru, L. Sacarescu, B. C. Donose, A. V. Nguyen, Polymer Chemistry **45**(18), 4240 (2007).
[5] A. Shishido, O. Tsutsumi, A. Kanazawa, T. Shiono, T. Ikeda, N. Tamai, Journal of Physical Chemistry B **101**, 2806 (1997).
[6] R. Enea, I. Apostol, V. Damian, N. Hurduc, I. Iordache, IOP: Conf. Ser. **100**, 012022 (2008).
[7] R. Enea, N. Hurduc, I. Apostol, V. Damian, I. Iordache, D. Apostol, J. Optoelectron. Adv. Mater. **10**(3), 541 (2008).
[8] P. C. Logofatu, I. Apostol, M.-C. Castex, V. Damian, I. Iordache, M. Bojan, D. Apostol, Proc SPIE 6617, 661717 (2007).
[9] I. Apostol, D. Apostol, V. Damian, I. Iordache, N. Hurduc, I. Sava, L. Sacarescu, I. Stoica, (2009), Proc. of SPIE **7366 73661U-1 – 8** (2009).
[10] Kevin G. Yager, Christopher J. Barrett, in Smart Light-Responsive Materials, edited by Yue Zhao and Tomiki Ikeda John Wiley & Sons, Inc., (2009).

*Corresponding author: victor.damian@inflpr.ro